Fusion Engineering and Design 195 (2023) 113960

Contents lists available at ScienceDirect

Fusion Engineering and Design

journal homepage: www.elsevier.com/locate/fusengdes

Nuclear scoping analysis of ITER bioshield top lid toward its preliminary design review

P. Martínez-Albertos [a,*], P. Sauvan [a], J. Bergman [b], M. Loughlin [b,1], Y. Le Tonqueze [b], M. Thompson [b], R. Juárez [a]

[a] Dept. Ingeniería Energética, Universidad Nacional de Educación a Distancia (UNED), C/ Juan del Rosal 12, Madrid 28040, Spain
[b] ITER Organization, Route de Vinon-sur-Verdon, CS 90 046, 13067 St. Paul Lez Durance Cedex, France

ARTICLE INFO

Keywords:
ITER
Electronics
Radiation transport
Shielding

ABSTRACT

During ITER operations, electronics located in the crane hall, which is above the tokamak, will be exposed to neutron and photon fields from both the plasma and the activated water. To protect the electronics, the implementation of dedicated shielding on the crane hall platform and the bioshield top lid is required. The design demands optimisation attending to constructability, weight limits, and radiation shielding requirements. This work evaluates eight shielding configurations by assessment of the neutron flux and dose accumulated over 4700 h of operation at 500 MW for electronics protection. This corresponds to a neutron wall load of 0.3 MW a/m^2 as specified in the ITER Project Specification. An intermediate-source approach has been followed with SRC-UNED, considering all relevant radiation sources while minimising the computational time required. Results were presented at the top lid Conceptual Design Review aiming to support decision-making. Further optimisation has since been performed to reach a top lid proposal for its Preliminary Design Review. All outcomes show that radiation levels above the north and south crane hall platforms are compatible with the critical electronics requirements.

1. Introduction

The construction of the ITER Tokamak Complex, the 7-story edifice at the heart of the scientific installation hosting the machine, has nearly finished. However, there are a few components that have not been built yet and whose designs are still evolving. Among them, two nuclear-important elements are the bioshield top lid and the crane hall platform shielding. They will separate the tokamak building (B11) from the crane hall, a huge and hollow room where cranes used to transport heavy components into the tokamak pit are stored (see Fig. 1). Continuous efforts are being made to optimise their designs attending to the following requirements:

- Radiation protection. Several radiation sources have been identified in the past as relevant contributions to the total radiation field in the ITER facility during operation: (i) the plasma source, comprising both 14.1 MeV neutrons from DT reactions, and prompt photons induced by these neutrons [1]; (ii) the activated water source, which includes the decay of ^{16}N, ^{17}N and ^{19}O in the water running through the Tokamak Cooling Water System [2]. Such sources could impact the efficiency of critical and non-critical electronics to be deployed above the crane hall platform (from now on referred to as L4 platform) on both the south and north sides. Dedicated radiation shielding is needed to ensure compliance with electronics limits, as shown in Table 1.
- Constructability. Given the span (~Ø30 m), the lid must be resistant and stiff enough to tolerate typical movements of the facility and be designed to withstand accidental scenarios (such as earthquakes, fire, blast, aircraft impact, etc.), whilst maintaining a confinement function. Ordinary concrete is preferred over borated heavy concrete as this is less dense and provides a stiffer behaviour. Additionally, a two-stage approach using precast concrete is preferred, removing the risk of temporary formwork, and pouring wet concrete above the tokamak.

* Corresponding author.
E-mail address: pablo.ma@ind.uned.es (P. Martínez-Albertos).
[1] Current address: Oak Ridge National Laboratory, One Bethel Valley Road, Oak Ridge, TN, USA

https://doi.org/10.1016/j.fusengdes.2023.113960
Received 4 May 2023; Received in revised form 3 August 2023; Accepted 11 August 2023
Available online 16 August 2023

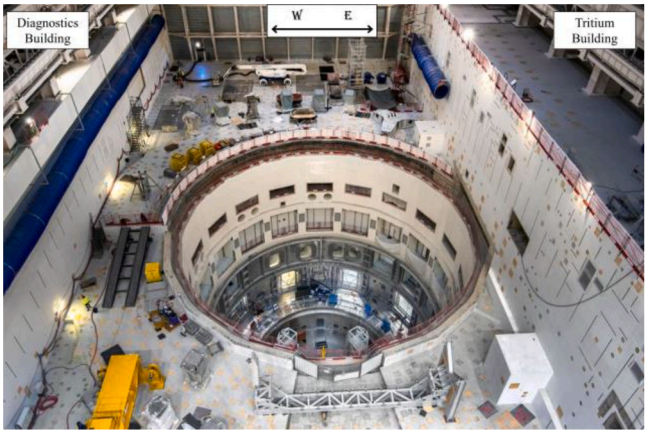

Fig. 1. View of crane hall slab and tokamak pit (November 2020). The top lid will sit above the pit.

Table 1
Limits of accumulated dose (in Gy) and neutron flux (in n cm^{-2} s^{-1}) for different ITER electronics groups.

System	Dose (Gy)	N. Flux (n cm^{-2} s^{-1})
Critical electronics	1	10
Non-critical electronics	10	100

- Weight limit. Based on current designs for the entire building, the maximum allowed weight for the bioshield top lid, and its shielding, must not exceed 3300 tonnes.

Previous studies have addressed the compatibility of the ITER radiation environment with the limit for electronics in different regions of the facility. However, the lid design and the shielding configuration considered corresponded to an outdated design not attending to current constructability requirements.

In this work, a scoping nuclear analysis has been performed to check the electronics limit compliance of several conceptual design configurations above the L4 platform and the top lid. Radiation zoning shall be also respected and has been considered during the design of the lid described in this study, although it has not been presented here. Previously defined engineering constraints have been considered for all configurations. Shielding efficiencies were analysed and results were proposed to support the decision-making of the Conceptual Design Review (CDR) of the top lid. Further work has been conducted to optimise one top lid configuration for its Preliminary Design Review (PDR). The dose accumulated over plasma operating time and neutron flux results within the crane hall are presented for all configurations.

2. Shielding configurations

Three different top lid concepts, shown in Fig. 2, have been considered in this study. They are:

- Lid-A: 130 cm thick combining normal concrete (2.2 g/cm^3) and borated heavy concrete (3.6 g/cm^3).
- Lid-B: 100 cm thick, made of borated heavy concrete.
- Lid-C: 130 cm thick lid made of normal concrete. It considers a concrete block on the bioshield south side.

All lids include a further layer of shielding material on top, described below.

The lid construction is conceived as a three-phase process, growing with the project stages. First, a precast element is inserted, sitting on existing bioshield walls. Second, more structural concrete is poured on top to upgrade shielding capabilities when needed. This solution eliminates the need for temporary formwork and the risk of wet concrete above the tokamak. Finally, non-structural shielding material, described below in this section, is included. This is done by fixing a steel square embedded plate grid to the lid (see Fig. 3), to later pour the shielding material within.

All cases have shielding above the L4 platform and either have or do

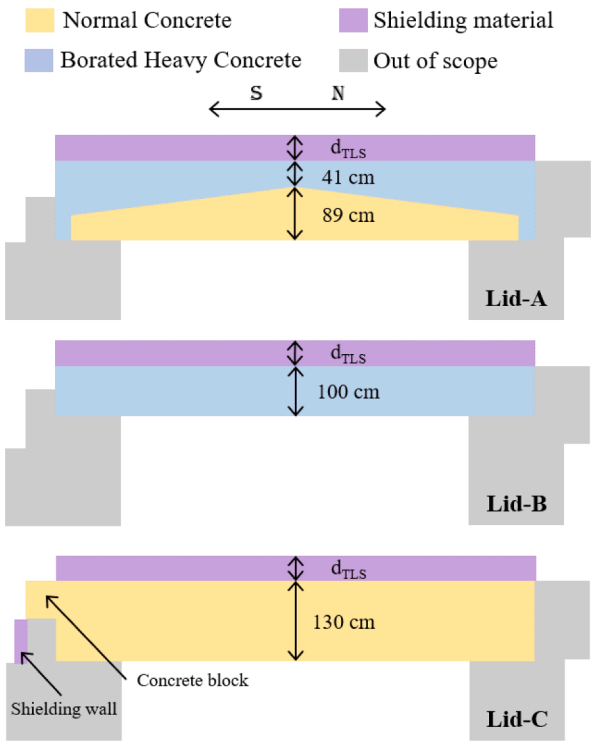

Fig 2. Schematical representation of top lid types considered. Colour legend and layers thicknesses are shown. Not to scale.

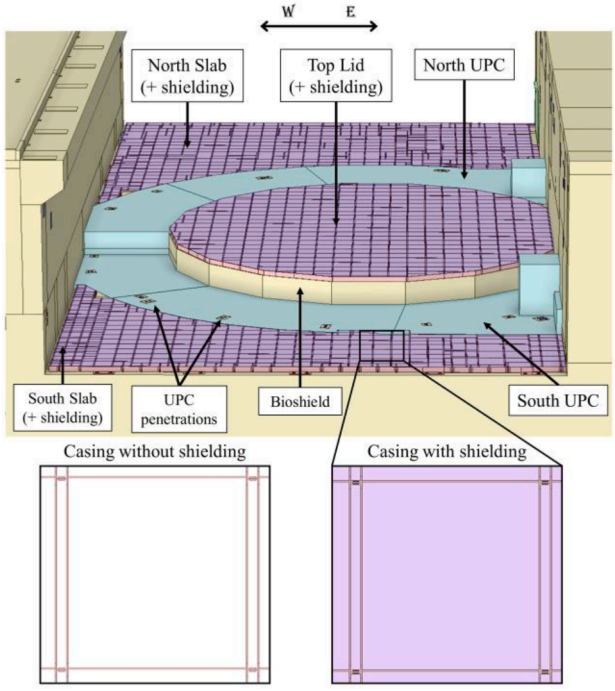

Fig. 3. View of CAD model of the L4 platform, UPC, and top lid with "partial" shielding scheme. Steel casings are shown.

not have shielding above the Upper Pipe Chase (UPC) (see Fig. 3). We refer to a "total" shielding scheme when both the L4 platform and the UPC are shielded, and "partial" when only the L4 platform is shielded.

Two field-castable materials, with high Boron content for neutron shielding, are considered for all shielding present in each configuration. Those are Shieldwerx-277Z-5 and Lemer-Pax Novashield borated Mortar 075, referred to as SWX and LP respectively.

A detailed geometric model of the shielding on top of the top lid, UPC and L4 platform is considered. It addresses the constructability solution of pouring shielding material into structural steel casings, leaving a 2–5 mm gap between shielding and casing (see Fig. 3).

Two extra cases are considered to assess the impact of (i) closing the gaps between shielding blocks, and (ii) changing the material to be used in the 13 penetration's backfilling in the UPC. NUVIA Nujoint 3130R is used instead of concrete.

The impact of the shielding around the bioshield in the south region above the UPC was addressed by including a shielding wall in a separate case (see Fig 2, Lid-C). This wall is the consequence of the 2 m vertical distance between the north and south platforms, seen in Figs 1–3.

The thickness of the shields above the L4 platform and the UPC remains constant for all cases, 43 cm and 10 cm respectively. The thickness of the shield above the top lid, d_{TLS}, depends on both the lid type and the shielding material. Its thickness is set as the maximum allowed to meet the lid weight limit.

Table 2 summarises all cases and shielding configurations considered in this study.

3. Intermediate sources approach

Several radiation sources contribute to the radiological environment at the crane hall. They consist of plasma neutrons, prompt photons from plasma neutrons, and photons and neutrons emitted from the decay of ^{16}N and ^{17}N present in the activated water running through several circuits of the Tokamak Cooling Water System [2].

Usually, evaluating the radiation levels produced by one source requires executing one calculation using a single geometry configuration. Due to the limited CPU time available, the number of radiation sources to be considered, and the number of shielding configurations to study, it was computationally unaffordable to launch independent MCNP [3] simulations for all scenarios. For this reason, these (primary) radiation sources were used to produce two intermediate sources, one for photons and one for neutrons, comprising only particles impacting on the crane hall. SRC-UNED methodology [4] has been used with such purpose.

Primary sources were used in the first simulation to record all particles reaching 3 independent planes which lay between the origin of primary sources and the crane hall, encapsulating it. These planes are $X = 1665$ cm, $Z = 1506$ cm and $Z = 1706$ cm and refer to ITER tokamak global coordinate system, which origin is in the centre of the tokamak. Ground level is at $Z = -148$ cm. The $X = 1665$ cm plane is located inside the east building of the Tokamak Complex (see Fig. 4). Z planes are located below the south and north L4 platforms respectively (see Fig. 5). Information is stored in a WSSA file which collects the energy, direction, and position of all particles reaching the selected planes. Such a file is used later to re-sample particles in a second simulation, which may consider a different shielding configuration of the top lid and crane hall shielding. The result is partial information: the radiation environment produced by particles reaching the crane hall due to a specific shielding configuration.

Intermediate sources are also used with the (reference) pre-concept shielding configuration of the top lid used in [1] for two reasons; (1) checking the validity of the intermediate sources and (2) estimating the radiation environment in the facility not affected by the top lid and crane hall shielding. This is done by subtracting results due to the intermediate sources from results obtained in a full calculation using all sources and a complete model of the tokamak complex [1]. This complementary information may then be added to the partial information provided by the intermediate sources with a different shielding configuration; the result is a radiation map in the whole facility due to the new shielding. A graphical representation of the approach is shown in Fig. 4.

This approach has led to possibility to perform a scoping analysis on a schedule compatible with ITER Project, saving approximately between 2 and 3 M CPU·h if extrapolating the computational time spent for the reference case with primary sources to all studied configurations.

Bear in mind that this approach does not modify the radiation environment outside the crane hall. This is affected by other sources or streaming paths and is included in the complementary information.

Table 2
Summary of shielding configurations considered.

Case	Lid	Shield	Material	Notes	d_{TLS} (cm)
Case 1	A	Partial	SWX		14.2
Case 2	A	Partial	LP		20.2
Case 3	B	Partial	LP		32.2
Case 4	B	Total	LP		32.2
Case 4a	B	Total	LP	Filled gaps	32.2
Case 4b	B	Total	LP	L4 backfill	32.2
Case 5	C	Partial	LP		77
Case 6	C	Partial	LP	LP wall	77

4. Methodology

Results have been tallied in single voxel meshes, shown in Fig. 5, which are 1 m above the top lid and the L4 platform. This is the anticipated location of the steel platform, not considered in this study, on top of which the electronic-containing cubicles will be deployed. Results show the shielding performance of the configurations from Table 2 concerning the compatibility of the critical electronics limit. Finer resolution 3D results were produced using superimposed meshes ($1 \times 1 \times 1$ m^3) for all cases to check the significance of single-voxel results.

The latest Tokamak Complex MCNP model [5] was used for all cases, modified to include the different shielding configurations studied. Space-Claim 2021 R1 [6] was used to modify, simplify and refurbish the CAD models of the shielding cases from Table 2. CAD to MCNP translation was performed using SuperMC [7,8].

A geometrical error debugging process was conducted for every shielding case until a loss particle rate of 10^{-9} was met. It comprised MCNP simulations in void mode with a spherical isotropic source. The sphere radius was chosen to be the minimum to cover the whole model.

SRC-UNED methodology is used to produce the intermediate sources (described in Section 3) from the primary sources from [1,2].

All calculations were run with D1SUNED v.3.1.4 [9]. Nuclear data considered for neutron transport corresponds to FENDL3.1c/d [10] and MCPLIB84 [11] for photon transport. Global variance reduction technique [12] is considered. Simulations were run until statistical errors dropped below 10%. A multiplicative safety factor of 2 is used following ITER Organization recommendations.

5. Results

Neutron flux and dose to silicon (from both neutron and photon contributions) in tallies from Fig. 5 are shown in Tables 3 and 4. Neutron flux values correspond to 500 MW operation (Fig. 6). Doses are accumulated over 4700 h of 500 MW (Fig. 7) (corresponding to a neutron wall load of 0.3 MW a/m^2 as specified in the ITER Project Specification).

For all configurations considered, approximately 95% of the dose results are due to photon contribution, mainly from the ^{16}N decay in the water circuits. The neutron flux is dominated by plasma neutrons, contribution of ^{17}N decay neutrons is negligible.

All configurations studied are compliant with the limits for critical electronics above the L4 platforms, both on the north and south tallies (where electronics will be deployed). Finer resolution 3D radiation maps support this conclusion for all cases, as may be seen in Figs. 8 and 9.

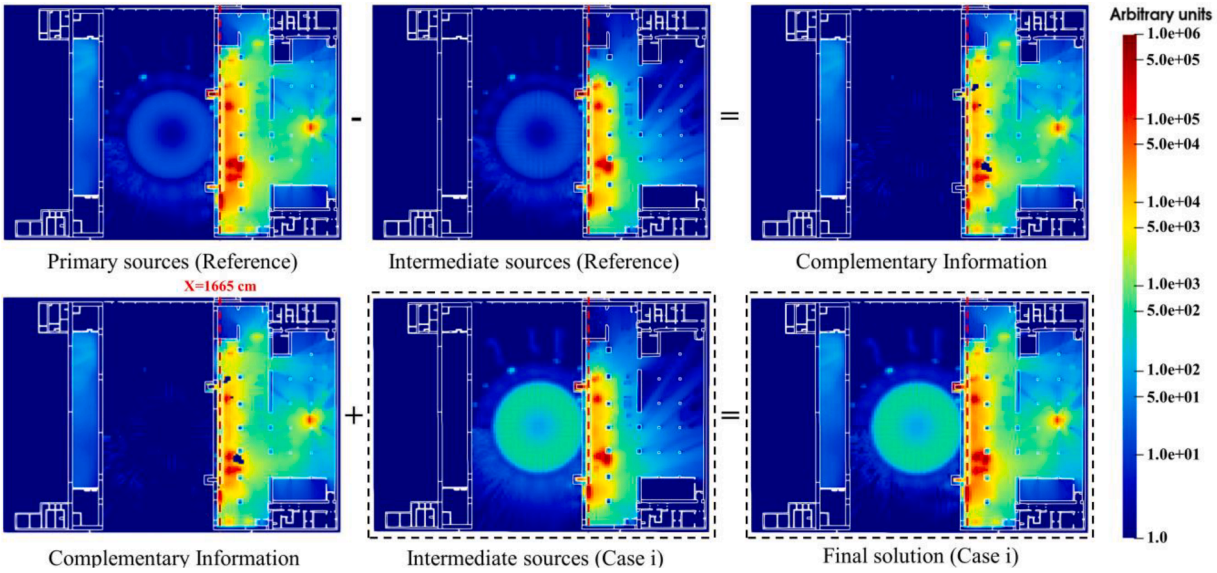

Fig. 4. Graphical representation of intermediate sources scheme in plane $Z = 2000$ cm, using dose to Silicon in arbitrary units. Black dashed boxes indicate maps that are calculated for all cases described in Table 2. Plane $X = 1665$ cm is shown with a red dashed line.

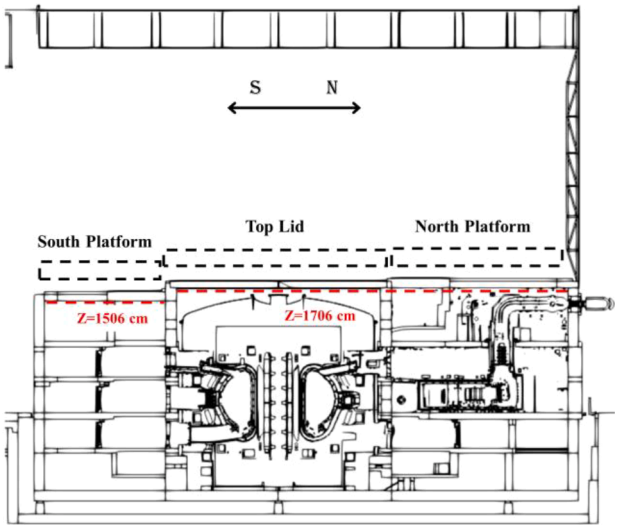

Fig. 5. B11 cross-section view ($x = 0$). Single-mesh tallies above L4 platforms and top lid are shown (approximate scale).

Table 3
Final neutron flux results, in n cm^{-2} s^{-1}, for all cases.

Neutron flux (n cm^{-2} s^{-1})	South platform	Top lid	North platform
Case 1	9.3	61	4.9
Case 2	5.8	35	2.7
Case 3	5.5	34	2.5
Case 4	5.0	33	2.4
Case 4a	4.9	32	2.2
Case 4b	5.1	33	2.4
Case 5	2.0	2.1	0.15
Case 6	1.1	2.1	0.14

The presence of hot spots within the south platform macro-tally is observed for both the accumulated dose and neutron flux for several cases. However, macro-tallies were found suitable, and slightly conservative, indicators of radiation conditions for electronics in the crane hall, as critical electronics will not be displayed at such short distance from the lid. Thus, such hot spots do not impact in the general conditions of electronics in the crane hall.

Table 4
Combined neutron-photon dose to Si accumulated over 4700 h of 500 MW ITER operation, in Gy, for all cases.

Accumulated dose in Si (Gy)	South platform	Top lid	North platform
Case 1	0.47	2.2	0.041
Case 2	0.47	2.1	0.039
Case 3	0.45	1.5	0.036
Case 4	0.40	1.5	0.035
Case 4a	0.39	1.5	0.035
Case 4b	0.38	1.4	0.033
Case 5	0.61	3.9	0.083
Case 6	0.23	3.9	0.083

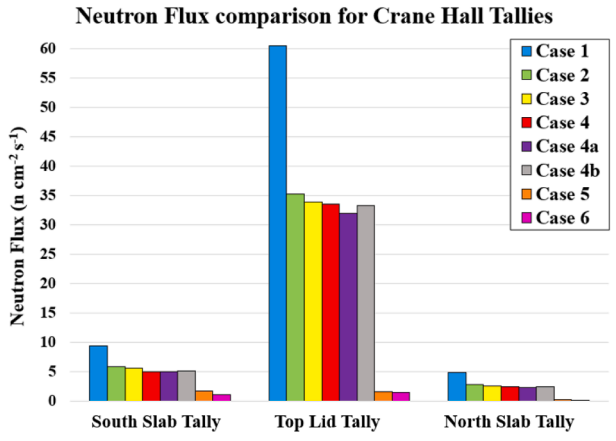

Fig. 6. Final neutron flux results, in n cm^{-2} s^{-1}, for all cases, in south and north platform and top lid macro-tallies.

In the case of the accumulated dose, values above 1 Gy are found for cases 1 to 5. For the neutron flux, values above 10 n cm^{-2} s^{-1} are observed for case 1 only. This phenomenon is due to the geometry weak point caused by the 2 m height difference between the top lid and south platform. Case 6 shielding wall addresses this issue.

The comparison of results from Cases 1 and 2 shows that Lemer-Pax is preferred over Shieldwerx as neutron shielding. 70% difference is seen

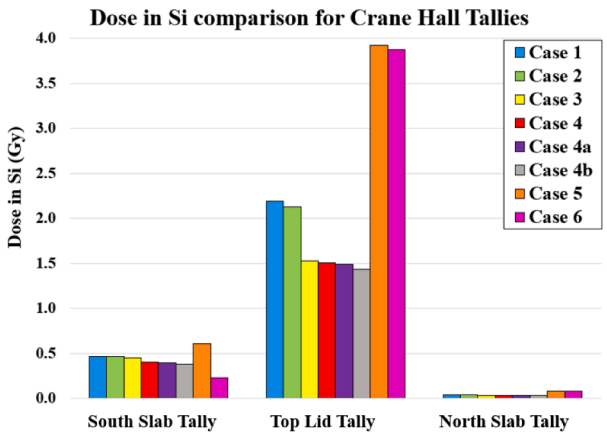

Fig. 7. Final Dose to silicon accumulated over 4700 h of 500 MW ITER operation, in Gy, for all cases, in south and north platform and top lid macro-tallies.

on average for all neutron flux tallies. There are no significant changes in dose to silicon.

Comparing results above the lid from Cases 2 and 3, it is seen that Lid-B performs slightly better than Lid-A for photon shielding (40% improvement in the dose). In terms of neutron shielding, they are equivalent.

Analysing results from Case 5, Lid-C, we see that the neutron flux over the lid is 22 times lower than in Case 3, Lid-B. However, the dose result is 2.5 times higher. This is produced by the reduction of borated heavy concrete in the lid, despite the increase of shielding material above, which is a shielding material targeting neutrons.

The LP wall around the bioshield considered in Case 6 considerably impacts results around its target area (south platform only due to the already mentioned 2 m vertical distance between north and south platforms). A 55% reduction for neutron flux and 37% for accumulated dose in Si is obtained in the south platform tally.

Considering Cases 3 and 4, the shielding above the UPC does not have a noticeable impact on either neutron flux or dose results. Very slight improvement may be seen on both nuclear quantities on the north platform tally. The main neutron and photon leakages are not coming from the UPC but from the lid.

Comparing cases 4 and 4a, it is seen that closing the 2–5 mm gaps between shielding and casing subtly impacts on tallied results. Neutron flux values are slightly more affected, as the gaps have been closed by filling them with Lemer-Pax, which is a neutron shielding material.

The change of material of UPC openings does not affect the global results, as may be seen if comparing cases 4–4b. However, a factor 10 local reduction is found.

6. Conclusions

This article describes a methodology for the assessment of shielding at ITER. In spite of the large physical size of the facility, the calculations were performed within a manageable timeframe. The estimated computational time saved is between 2 and 3 M CPU h. The bioshield top lid and the crane hall platform shielding require optimisation to protect critical electronics. In this study, a scoping analysis considering both plasma and activated water radiation sources was performed attending to constructability, weight limits and radiation shielding requirements. The main conclusions are:

- The radiation environment in the crane hall during operation includes both neutron and photon fields from the plasma and activated water.
- Lemer-Pax is preferred over Shieldwerx as a neutron shielding material.
- Both Lid-A and Lid-B designs (with LP shielding above) are equivalent in terms of neutron shielding. Lid-B is slightly more efficient against photons.
- Lid-C design (with LP shielding above) has the highest neutron shielding efficiency. On the contrary, it presents the lowest photon shielding efficiency due to the removal of (borated) heavy concrete.
- The LP wall around the bioshield has a relevant impact on results around its target area.
- The shielding above the UPC does not have a noticeable impact.
- NUVIA Nujoint on L4 openings backfills reduces radiation levels locally.
- Due to the combined effect of neutron and photons fields, a balance of high-density materials (such as heavy concrete) and borated materials with a high fraction of low atomic elements (such as LP) is preferred.

All cases considered are compatible with the ITER limit for critical

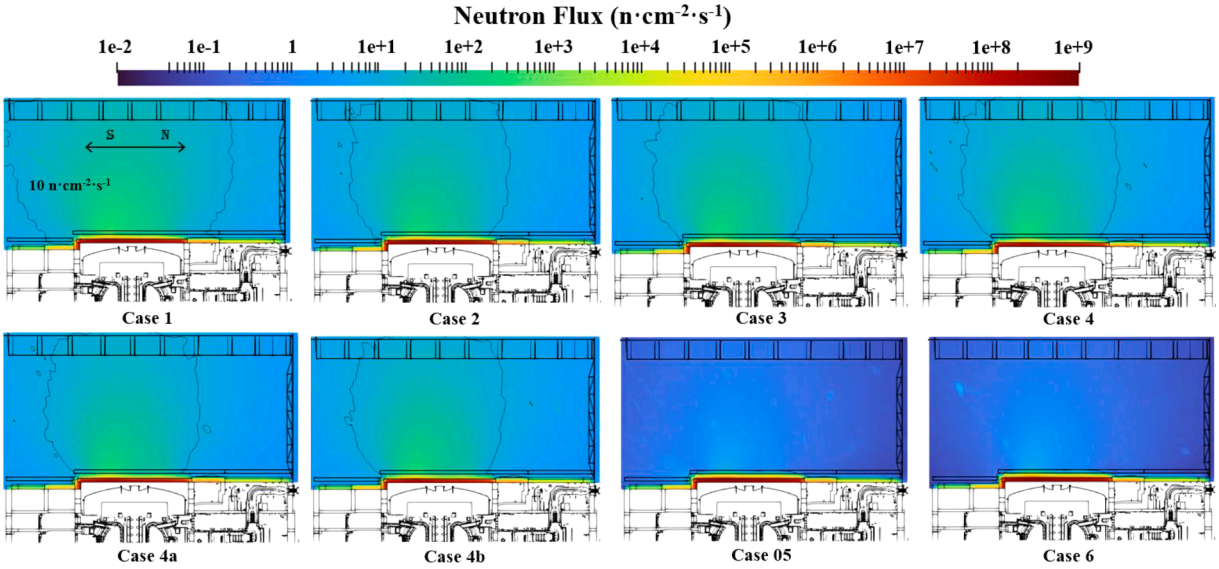

Fig. 8. Neutron flux (in n cm^{-2} s^{-1}) in the crane hall, at plane $x = 0$ cm, for all studied cases. Black boxes indicate the macro tallies used. From left to right: south platform, top lid and north platform. 10 in n cm^{-2} s^{-1} iso-surface is shown.

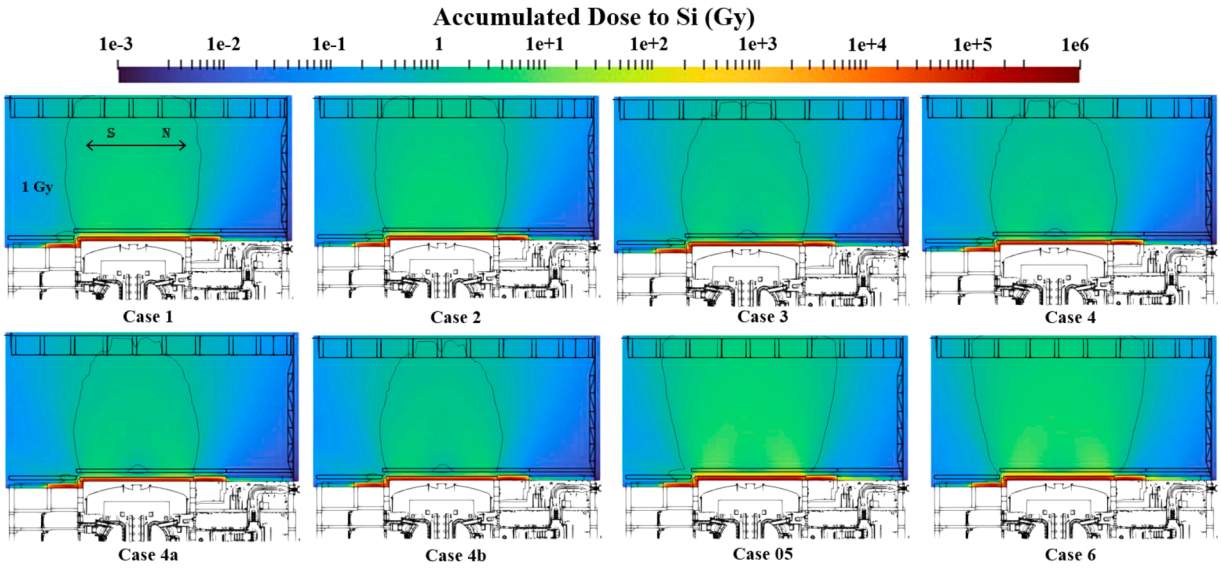

Fig. 9. Dose to Silicon accumulated over 4700 h of 500 MW plasma operation (in Gy) in the crane hall, on the plane $x = 0$ cm, for all studied cases. Black boxes indicate the macro tallies used. From left to right: south platform, top lid and north platform. 1 Gy iso-surface is shown.

electronics in both the north and south platform, where these systems will be deployed. Further optimization of the lid shielding design will be needed to balance the effect of both neutrons and photons on the radiation environment in the crane hall.

CRediT authorship contribution statement

P. Martínez-Albertos: Methodology, Formal analysis, Writing – original draft. **P. Sauvan:** Methodology, Formal analysis. **J. Bergman:** Resources, Validation, Writing – review & editing. **M. Loughlin:** Project administration, Validation, Writing – review & editing. **Y. Le Tonqueze:** Project administration, Validation, Writing – review & editing. **M. Thompson:** Resources. **R. Juárez:** Formal analysis, Funding acquisition, Supervision, Writing – review & editing.

Declaration of Competing Interest

The authors declare that they have no known competing financial interests or personal relationships that could have appeared to influence the work reported in this paper.

Data availability

The authors are unable or have chosen not to specify which data has been used.

Acknowledgements

This work has been carried out partially within the framework of the EUROfusion Consortium, funded by the European Union via the Euratom Research and Training Programme (Grant agreement no. 101052200 —EUROfusion). Views and opinions expressed are however those of the author(s) only and do not necessarily reflect those of the European Union or the European Commission. Neither the European Union nor the European Commission can be held responsible for them.

This work has been performed under the ITER contract IO/20/CT/6000000345 between UNED and ITER Organization.

We appreciate the support given by: MINECO for the funding of Juan de la Cierva-incorporación program 2016; and the funding under I+D+i-Retos Investigación, Prj. ENE2015-70733R; Comunidad de Madrid under I+D en Tecnologías, Prj. TECHNOFUSIÓN (III)-CM, S2018/EMT-4437; Escuela Técnica Superior de Ingenieros Industriales (UNED) of Spain, project 2023-ETSII-UNED-03; and UNED for the funding of the predoctoral contracts (FPI) and of the open access publishing.

References

[1] R. Juárez, G. Pedroche, et al., A full and heterogeneous model of the ITER tokamak for comprehensive nuclear analyses, Nat. Energy 6 (2021) 150–157.
[2] M. De Pietri, J. Alguacil, et al., Integral modelling of the ITER cooling water systems radiation source for applications outside of the bio-shield, Fusion Eng. Des. 171 (2021), 112575.
[3] J.E. Sweezy, X-5 Monte Carlo and X-5 Data Team, MCNP Manual. MCNP – A General Monte Carlo N-Particle Transport Code, Version 5, LA-UR-03-1987, (2003).
[4] J.P. Catalan, F. Ogando, et al., Development of radiation sources for nuclear analysis beyond ITER bio-shield: SRC-UNED code, Comput. Phys. Commun. 275 (2022), 108309.
[5] P. Martínez-Albertos, P. Sauvan, et al., Assessment of ITER radiation environment during the remote-handling operation of in-vessel components with D1SUNED, Sci. Rep. 13 (2023) 3544.
[6] Ansys® Space Claim, 2021 Release 1.
[7] Y. Wu, J. Song, H. Zheng, et al., CAD-based monte carlo program for integrated simulation of nuclear system SuperMC, Ann. Nucl. Energy 82 (2015) 161–168.
[8] Y. Wu, F.D.S. Team, CAD-based interface programs for fusion neutron transport simulation, Fusion Eng. Des. 84 (2009) 1987–1992.
[9] P. Sauvan, R. Juárez, et al., D1SUNED system for the determination of decay photon related quantities, Fusion Eng. Des. 151 (2020), 111399.
[10] R.A. Forrest, R. Capote, et al., FENDL-3 Library Summary Documentation, International Atomic Energy Agency, Vienna, Austria, 2012. INDC(NDS)-0628.
[11] M.C. White, "Further Notes on MCPLIB03/04 and New MCPLIB63/84 Compton," LA UR 12 00018.
[12] A.J. van Wijk, An easy to implement global variance reduction procedure for MCNP, Ann. Nucl. Energy 38 (2011) 2496–2503.